

## Efficient Peroral Delivery of Insulin via Vitamin B<sub>12</sub> Modified Trimethyl Chitosan Nanoparticles

Zhiyang Ke, Han Guo, Xi Zhu, Yun Jin, Yuan Huang

Key Laboratory of Drug Targeting and Drug Delivery, Ministry of Education, Sichuan University, Chengdu, P.C. China

Received, December 6, 2014; Revised, April 3, 2015; Accepted, May 5, 2015; Published, May 6, 2015.

**ABSTRACT-PURPOSE:** We investigated the effect of vitamin B<sub>12</sub> (VB<sub>12</sub>) modification on the insulin absorption from trimethyl chitosan(TMC) nanoparticles (NPs) under the influence of mucus. **METHODS:** TMC and TMC-VB<sub>12</sub> were synthesized and insulin loaded TMC/TMC-VB<sub>12</sub> nanoparticles were prepared and characterized. Modified and unmodified nanoparticles were studied with Caco-2/HT29-MTX cell model and ligated rat ileum loop. **RESULTS:** Compared with unmodified NPs, VB<sub>12</sub> modified NPs showed significantly higher drug internalization in Caco-2/HT29-MTX cell model. The internalization mechanism via VB<sub>12</sub> mediation included caveolae and clathrin-mediated endocytosis pathway. Meanwhile, an increased transportation of drugs was observed for VB<sub>12</sub> modified NPs, possibly due to the ligand-receptor interaction via an intrinsic factor-dependent fashion. Although the uptake and transport of VB<sub>12</sub> modified NPs could be partially influenced by mucus, they still showed higher drug permeation through Caco-2/HT29-MTX co-cultured cells than unmodified NPs in the presence or absence of mucus. Moreover, in situ study in ligated rat ileum loop demonstrated that VB<sub>12</sub> modified nanoparticles could reduce the residual insulin in intestinal lumen (0.59 times) and increase their absorption in epithelial tissue (4.8 times) compared with the unmodified ones. **CONCLUSION:** VB<sub>12</sub> modified trimethyl chitosan nanoparticle is a promising carrier for peroral delivery of insulin.

This article is open to **POST-PUBLICATION REVIEW**. Registered readers (see "For Readers") may **comment** by clicking on ABSTRACT on the issue's contents page.

### INTRODUCTION

Oral delivery of protein drugs is a fascinating challenge which has been explored by pharmaceutical scientists for decades (1-3). The barriers for efficient oral absorption of these biomolecules primarily include rapid enzymatic degradation in gastro-intestinal (GI) tract and the intrinsic low permeability across the intestinal epithelium. Nanoparticles (NPs) have been proposed as promising vehicle for oral drug delivery by protecting the protein drugs against harsh environment of the GI fluid. More importantly, NPs can be internalized by the enterocyte through various mechanisms, thus enhancing the permeation of the loaded drug through epithelium.

More recently, NPs modified with ligands which can specifically bind to different cells on epithelium were suggested as a strategy to further enhance the permeation and delivery efficacy (3). These ligands can either increase the accumulation of the NPs on the surface of the epithelium or mediate a certain pathway of internalization via the ligand-receptor binding. In a recent report of our group, a peptide ligand,

which can specifically bind to goblet cell, can effectively increase the interaction of NPs to the intestinal epithelium (4). Furthermore, some ligands were even identified to mediate direct transcytosis, by which a 15% bioavailability of loaded insulin could be achieved by the ligand modified polymeric NPs (5). However, though promising, limited number of the ligands have been used due to their chemical nature and unwarrantable bioactivity *in vivo* (6). For example, transferrin, an iron-binding glycoprotein, was reported to induce clathrin-dependent endocytosis. However, the protein nature and the large molecular weight (~77 KDa) largely limited its convenience and efficacy of conjugation onto the surface of NPs (7).

Vitamin B<sub>12</sub> (VB<sub>12</sub>), also called cobalamin, a water-soluble vitamin with a key role in the normal functioning of the brain and nervous system, is efficiently absorbed in GI tract by a

---

**Corresponding Author:** Professor Yuan Huang. Key Laboratory of Drug Targeting and Drug Delivery, Ministry of Education, Sichuan University, No. 17. Block 3. Southern Renmin Road, Chengdu, P.C. China; E-mail: huangyuan0@163.com

complex dietary uptake pathway. Application of VB<sub>12</sub> for the delivery of pharmaceutical agents has received attention since 1970s (8). During its uptake process, VB<sub>12</sub> firstly binds to salivary haptocorrin in stomach (9,10), and subsequently binds to intrinsic factor (IF) in intestine. VB<sub>12</sub> can then be transcytosed through epithelium by IF-receptor mediated pathway. Different protein and peptide drugs have been successfully conjugated with VB<sub>12</sub> to facilitate their oral absorption (11-13). However, this conjugation approach faces several limitations. First, the amount of VB<sub>12</sub> ingesting per day can be plateaued (5-30µg for adult) which limits the maximal delivery of pharmaceutical agents if the VB<sub>12</sub> and drugs were conjugated at 1 to 1 ratio (8); secondly, chemical conjugation could harm the bioactivity of the conjugated agents (14).

Therefore, in this study, we reported a VB<sub>12</sub> conjugated N-trimethyl chitosan (TMC) nanoparticles which were prepared by a relatively modest approach of self-assembly. Insulin was chosen as model drug which can be efficiently loaded with high encapsulation efficiency. By this approach, we expect enhanced amounts of loaded drugs can be delivered across the epithelium by combining the effect mediated by VB<sub>12</sub> and the permeation enhancing effect of TMC which have been explicitly demonstrated (4, 15-17). The efficacy of the VB<sub>12</sub> NPs for insulin delivery was investigated *in vitro* and *in situ*. Furthermore, the influence of mucus, which may influence the binding of the NPs with the epithelial cells, was also studied.

## MATERIALS AND METHODS

### Materials

Chitosan (Mw = 400 kDa, deacetylation degree > 90.0%) was purchased from Aokang Biotechnology Ltd. (Shandong, China). Porcine insulin (30 IU/mg) (INS) was from Wanbang Bio-Chemical Co., Ltd. (Jiangsu, China). Vitamin B<sub>12</sub> (cobalamin) was a kind gift from Hebei Yuxing Bio-engineering Co., Ltd. (Hebei, China). Succinic anhydride, pluronic F-68 and sodium tripolyphosphate were from Shanghai Chemical Reagent Company (Shanghai, China). Fluorescein isothiocyanate (FITC), intrinsic factor (IF) from porcine gastric mucosa, and 3-(4,5-dimethyl-thiazol-2-yl)-2,5-diphenyl tetrazolium bromide (MTT) were all purchased from Sigma-Aldrich (St. Louis, MO, USA). Caco-2 cells were gained from institute of Biochemistry and Cell Biology (Shanghai, China). HT29-MTX

cell line was a kind gift from Dr. Thecla Lesuffleur (INSERM, Paris, France). N-Acetyl-L-Cysteine was obtained from Aladdin Chemistry Co., Ltd. (Shanghai, China). 1-[3-(Dimethylamino)propyl-3-ethylcarbodiimide hydrochloride (EDC·HCl) was gained from Meapeo Co., Ltd. (Shanghai, China). N-Hydroxy succinimide (NHS), N-methyl pyrrolidone, iodomethane were all obtained from Kelong chemical Co., Ltd (Chengdu, China). Other agents were all analysis grade.

### Synthesis of TMC and TMC-SA-VB<sub>12</sub>

TMC was synthesized according to the schematic route in **Figure 1**. Briefly, chitosan (CS) and methyl iodide were reacted in a strong base environment (sodium hydroxide, NaOH) using N-methyl pyrrolidone as solvents. The reaction was proceeded for 90min at 60 °C. The obtained product was precipitated using ethanol and the precipitation was dissolved in moderate amount of water and the iodide was exchanged by chloride in ethanol contains hydrochloric acid. Then the product was purified via dialysis (Mw range from 8000 Da to 14000 Da) in water and lyophilized (SNL216V, Savant Instruments Inc., NY, USA) 36 hours to achieve white fluffy TMC. The degree of quaternization (DQ) was calculated from the integration of <sup>1</sup>H nuclear magnetic resonance (<sup>1</sup>H NMR, UNITY INOVA-400, Varian Inc., CA, and USA) (18).

For the synthesis of VB<sub>12</sub> conjugated TMC, VB<sub>12</sub> was firstly modified with succinic anhydride as a linker. VB<sub>12</sub> (36.9 µmol) was dissolved in 10 mL of anhydrous dimethylsulfoxide containing succinic anhydride (SA, 1.8 mmol) and 4-dimethylamiopyridine (19.0 µmol). After 24 h of reaction at room temperature, the mixture was precipitated with anhydrous acetone for 3 times and then dried in vacuum. The obtained VB<sub>12</sub>-SA was identified by electrospray ionization mass spectrometry (ESI-MS). Subsequently TMC was conjugated with VB<sub>12</sub>-SA via amide bond formed among the residual primary amino groups in TMC and carboxyl groups in VB<sub>12</sub>-SA. The TMC-SA-VB<sub>12</sub> was identified by <sup>1</sup>H NMR and ultraviolet (UV) spectra. The degree of VB<sub>12</sub> substitution was determined by UV spectrophotometer (λ = 361 nm) using a calibration curve prepared with standard solutions of VB<sub>12</sub> (19). Fluorescein isothiocyanate-Porcine insulin (FITC-INS) was synthesized as reported (20).

High performance liquid chromatography (HPLC) assay was utilized to determine the purity

of products. The HPLC system (Agilent Technology 1200 series) was composed of a 150mm× 4.6 mm reversed-phase  $^{18}$ C column, with a UV spectrophotometer. 25% methanol was used as mobile phase with a flow rate of 0.8mL/min and detected at 361nm.

### Preparation of nanoparticles

The fluorescent INS-loaded NPs were prepared by polyelectrolyte ionotropic gelation. Briefly, FITC-INS (1 mg/mL), sodium tripolyphosphate (1 mg/mL) and pluronic F-68 solution (6 mg/mL) were mixed at a ratio of 3:5:5 (v/v). Then the pre-mixed solution was added drop-wisely to TMC or TMC-SA-VB<sub>12</sub> aqueous solution (0.8 mg/mL) at a ratio of 2:1 (v/v) and the NPs (TMC INS NPs and TMC-SA-VB<sub>12</sub> INS NPs) was termed as T NPs and VB<sub>12</sub>-T NPs, respectively. The mixture was stirred at room temperature for 20 min, yielding a yellow-brown suspension. The resultant suspension was ultracentrifuged at 14,000 rpm for 30 min at 4°C. The supernatant was separated for the determination of entrapment efficiency and the NPs in pellet were resuspended

for further use.

The structure integrity of FITC-INS after NPs fabricating procedure was determined using sodium dodecyl sulfate-polyacrylamide gel electrophoresis (SDS-PAGE). Electrophoresis equipment (Jun Yi, Beijing, China) composed of a vertical slab minigel cell was used. 8  $\mu$ l of FITC-INS, plain NPs, T NPs and VB<sub>12</sub>-T NPs were loaded respectively on 5% upper stacking gel and were separated with 17.5% lower resolving gel in tris-glycine electrophoretic buffer (pH 8.3). Polyacrylamide gels were run for approximately 3 h at 80V. Afterwards, the gel was stained with coomassie brilliant blue (G-250) for 2 h to reveal the protein. Destainer was a mixture of glacial acetic acid, methanol and distilled water (2:9:9 v/v).

### Characterization of NPs

The particle size and zeta potential of T NPs and VB<sub>12</sub>-T NPs were measured by dynamic light scattering (DLS, NanoZS90 nanoseries, Malvern Instruments, UK) at the angle (90°) with a 15s acquisition time at 25°C. Atomic force

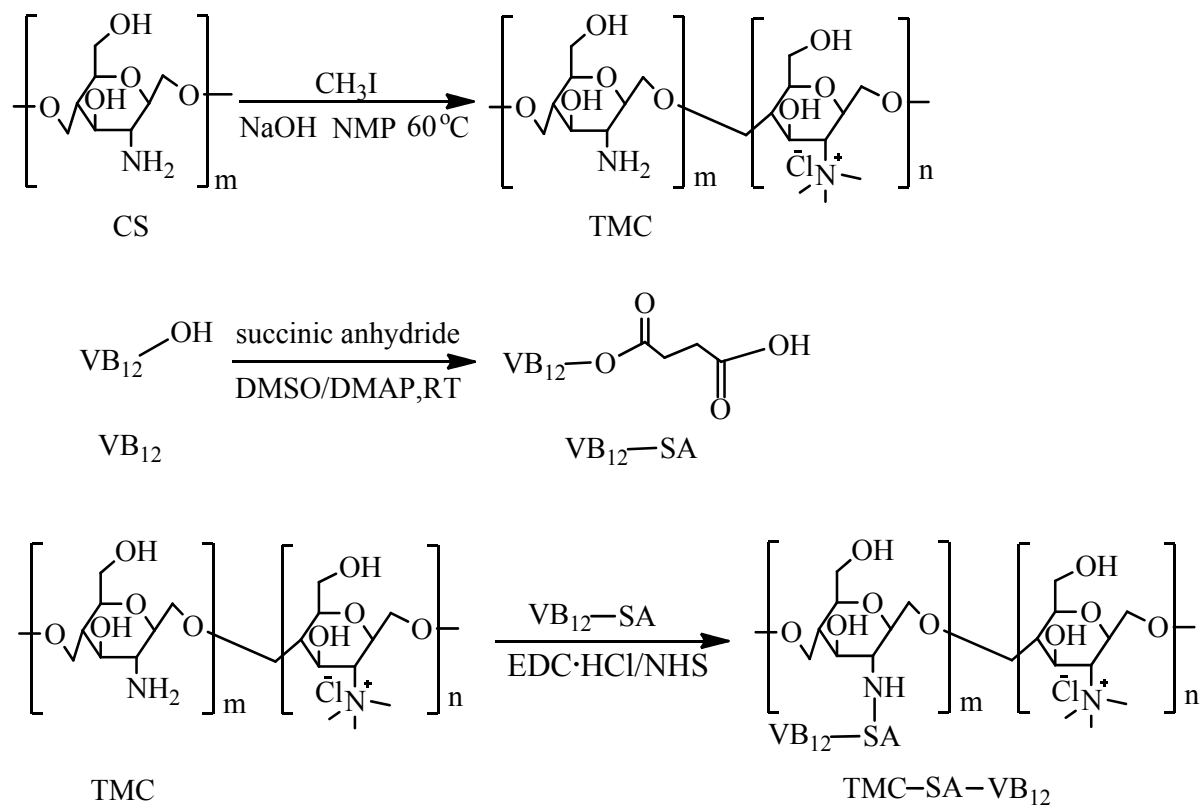


**Figure 1.** Synthesis of TMC and TMC-SA-VB<sub>12</sub>.

microscopy (AFM) images of the NPs were collected in air with a Nanoscope III (Digital Instruments, Santa Barbara, USA) operating in tapping mode (21) for the investigation of the morphology.

For evaluation of entrapment efficiency (EE%) and drug loading capacity (DL %), amount of free FITC-INS in the supernatant was determined by fluorospectrophotometer (Shimadzu Corp., Tokyo, Japan). The excitation and emission wavelengths were set at 488 and 516 nm, respectively. EE % and DL % of FITC-INS loaded NPs were calculated according to the following equations:

$$EE\% = \frac{\text{total amounts of drugs} - \text{amounts of free drugs}}{\text{total amounts of drugs}} \times 100\%$$

$$DL\% = \frac{\text{total amounts of drugs} - \text{amounts of free drugs}}{\text{NPs weight}} \times 100\%$$

#### Cell culture

Caco-2 and HT29-MTX cells were cultured in Dulbecco's Modified Eagle Medium (DMEM) with 10% fetal bovine serum, 1% non-essential amino acids, 1% L-glutamine, penicillin (100 IU/mL) and streptomycin (100 mg/mL). The cells were harvested at 80–90% confluence and seeded at a mixture of 1:1 ratio onto 96-well plates (Corning, NY, USA), and incubated for 2 days before cytotoxicity tests and 7 days before uptake studies. For transport assays, the cell suspensions were seeded onto the Transwell® chambers consisting of polycarbonate membrane (0.4 µm in pore size, 0.33 cm<sup>2</sup> of cell growth area, Costar Inc., NY, USA). The cells were allowed to grow and differentiate for 21 days before use (22).

#### Cytotoxicity assays

MTT assays were selected to evaluate the cytotoxicity of NPs. Prior to the test, cells were incubated with 100 µl of FITC-INS, T NPs or VB<sub>12</sub>-T NPs in Hank's balanced salt solution (HBSS) for 4 h (concentration of FITC-INS was 50, 100, 200, 300 and 400 µg/mL, pH7.4). Subsequently, samples were removed and the cells were rinsed with PBS followed by incubating with 200 µl of medium containing 0.5 mg/mL of MTT. Then the medium was replaced by 200 µl of dimethylsulfoxide to dissolve the formazan crystals formed by viable cells. Absorbance was measured at 570 nm using

Varioskan Flash (Thermo Fisher Scientific, MA, USA). HBSS was used as reference for 100% cell viability. Sodium dodecyl sulfate was chosen as positive control at a concentration of 50µg/mL.

#### Intracellular uptake of NPs on Caco-2/HT29-MTX co-cultured cell model

In order to estimate intracellular uptake of NPs and the relevant mechanisms, an *in vitro* uptake experiment was performed using Caco-2/HT29-MTX co-cultured cells.

Prior to the studies, the medium was replaced with pre-warmed HBSS to equilibrate at 37 °C for 30 min. The cells were then incubated with 100µl of FITC-INS, T NPs or VB<sub>12</sub>-T NPs in HBSS for 2 h (concentration of FITC-INS was 50, 100, 200, 300 and 400 µg/mL) at 37 °C. Subsequently, the cells were washed with ice-cold PBS and lysed with lysis buffer containing 1% triton X-100, 50 mM

4-(2-hydroxyethyl)-1-piperazineethansulfonic acid (HEPES, pH 7.4), 150 mM NaCl, 2 mM Na<sub>3</sub>VO<sub>4</sub>, 100mM NaF, 100 units/mL aprotinin, 20 mM leupeptin and 0.2 mg/mL phenylmethanesulfonyl fluoride. Then the cell associated fluorescence and proteins were determined by Varioskan Flash and bicinchoninic acid assay kit (KeyGen Biotech Co., Ltd., Nanjing, China), respectively. The amounts of uptake drugs were expressed as the quantity of FITC-INS associated with 1 mg of total cellular protein.

For the evaluation of the influence of mucus layer, the cells were pre-incubated with 10 mM N-acetyl-L-cysteine (dissolved in HBSS) for 60 min at 37 °C to remove the mucus. Then the uptake study was performed as described above.

To further clarify the effect of VB<sub>12</sub> as ligand and identify the internalization mechanism of NPs by co-cultured cells, the uptake study was performed with different inhibition agents. (i) To study the competitive inhibition effect of free VB<sub>12</sub>, cells were pre-incubated with VB<sub>12</sub> (5 mg/mL) in the cell culture medium for 1 h, rinsed twice with HBSS and incubated with the NPs suspension for 3h at 37 °C. (ii) To investigate the effect of desulfurization, cells were incubated with 35 mM sodium chlorate in cell culture medium for 48 h before incubated with the NPs suspensions (23). (iii) To study the inhibition effect of clathrin endocytosis, cells were incubated with 10 µg/mL chlorpromazine dissolved in NPs suspension and treated for 3h at 37 °C. (iv) To study the inhibition effect of caveolae endocytosis, cells were incubated with 1

$\mu\text{g/mL}$  filipin dissolved in NPs suspension and treated for 3h at 37 °C (24). In addition, the control samples were conducted at 37 °C for 3 h without any treatment. The results of the inhibition tests were presented as the percentage of that internalized in control.

### Transcellular permeation study

Co-cultured cell monolayer seeding on Transwell® inserts was utilized for mimicking the intestinal epithelium with both epithelial cells and mucus layer. Transepithelial electrical resistance (TEER) of the monolayer was measured using a Millicell-ERS (Millipore, MA, USA) to determine the integrity formation of the monolayer before the experiment. Typical TEER values exceeded 550  $\Omega \cdot \text{cm}$  (25).

Prior to the transport experiments, the medium was replaced with pre-warmed HBSS which equilibrated with cells at 37 °C for 30 min. Then 200  $\mu\text{L}$  of NPs (contain 300  $\mu\text{g/mL}$  FITC-INS) in HBSS were added to the apical chamber. At every determined time intervals (0.5, 1, 2 and 3 h), 200  $\mu\text{L}$  of samples were withdrawn from the basolateral chamber and equal volumes of fresh HBSS were added. The amounts of transported FITC-INS were determined by fluorospectrophotometer and the accumulative transport amounts were calculated. TEER measurements were also performed during the permeation experiment to assess the effects of T NPs and VB<sub>12</sub>-T NPs on the opening of tight junction during the transport experiment.

To investigate the influence of mucus, the mucus layer was removed prior to the experiment as described above and permeation study of the NPs was performed. To investigate the role of VB<sub>12</sub> on the transport of NPs, experiment was also performed with the addition of free VB<sub>12</sub> (5 mg/mL) or/and IF (200IU/mL). Experiments were conducted under identical conditions with T NPs.

### Absorption studies in the ligated intestinal loops

The *in situ* absorption of drugs was evaluated using the ligated intestinal loops model. All experiments were approved by the Institutional Animal Care and Use Committee of Sichuan University. Male Sprague Dawley rats (200±20g, Laboratory Animal Center, Sichuan University) were fasted overnight before experiments but allowed free access to water. The rat was anesthetized with pentobarbital sodium (40

mg/kg), and then 4-cm sections of ileum from small intestinal loop were made and ligated at both ends. 0.2 mL of FITC-INS, T NPs or VB<sub>12</sub>-T NPs suspension (concentration of FITC-INS was 300  $\mu\text{g/mL}$ ) were injected into the loop. 3 h later, rat was sacrificed by cervical dislocation and the section of each loop was removed. The intestinal loop was washed with a certain amount of PBS and the mucus was gently collected by a spatula. The remained tissue was then digested with 10% NaOH solution. FITC-INS in collected PBS, mucus and digested tissue were quantified by fluorospectrophotometer.

### STATISTICAL ANALYSIS

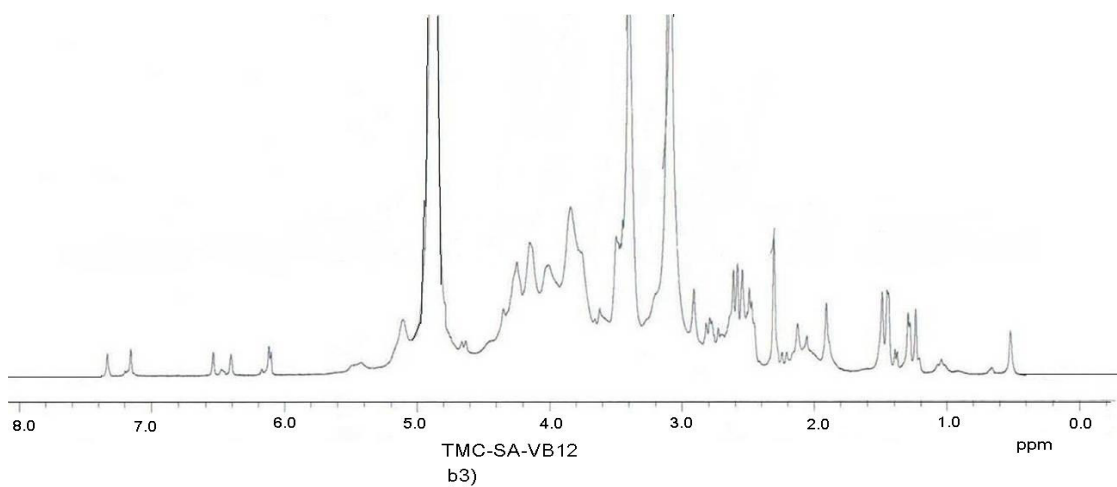
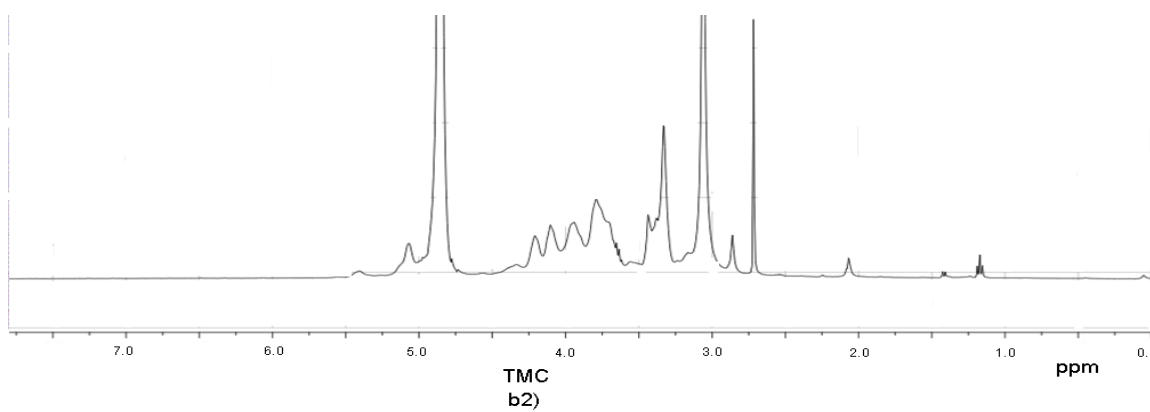
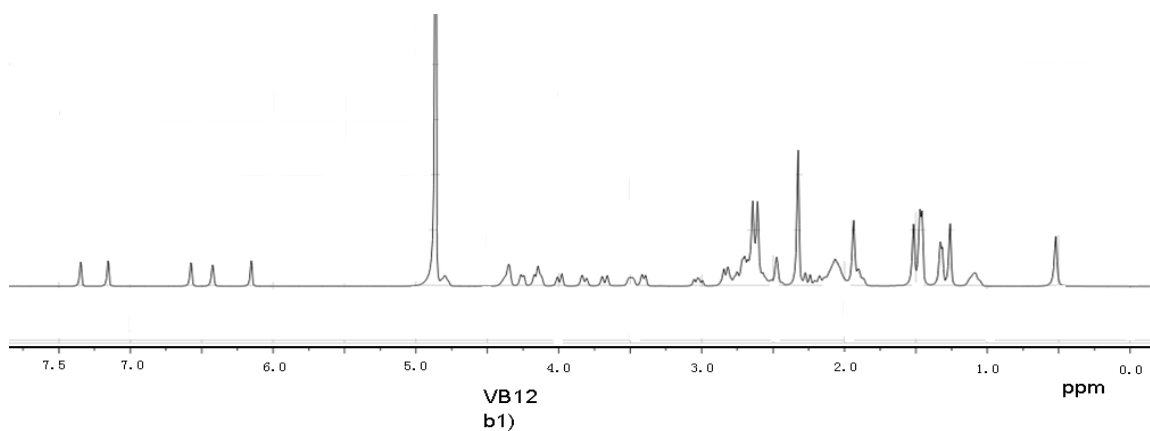
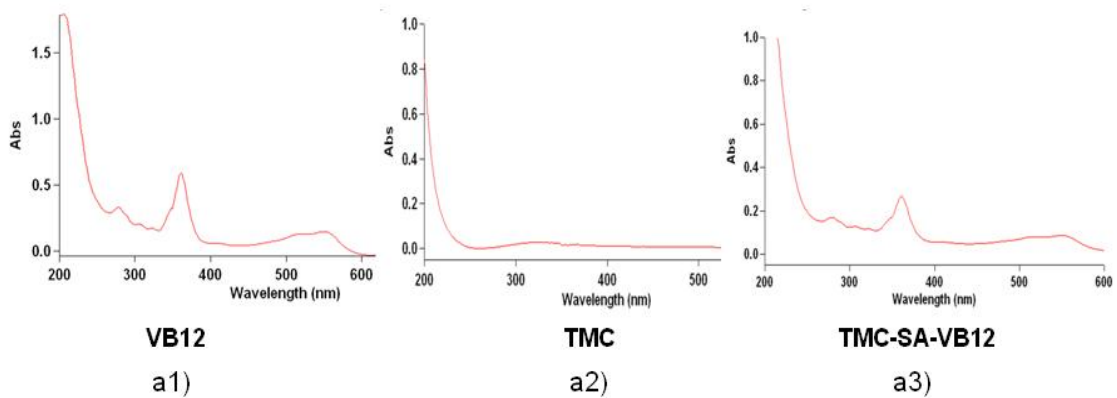
Data were reported as mean±standard deviation from 3 to 5 independent experiments. Statistical significance between mean values was calculated using independent sample t-test and one-way analysis of variance (ANOVA) with Dunnett's T3 post hoc test (SPSS 17.0, SPSS, Inc.). Probability values <0.05 were considered significant.

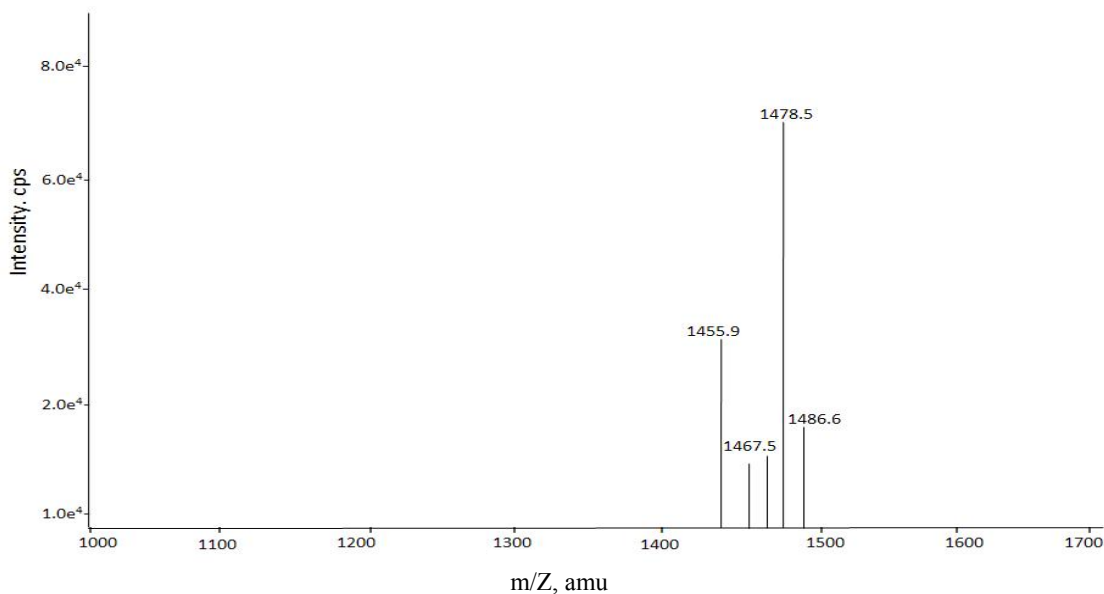
### RESULTS

#### Characterization of synthesized polymers

TMC with a DQ of 16.9% was synthesized and characterized by <sup>1</sup>H NMR (**Figure 2 b2**). <sup>1</sup>H NMR(400 MHz, D<sub>2</sub>O):  $\delta$  5.7~4.7 (s, 1H H1'), 3.38 (s, 9H N<sup>+</sup>(CH<sub>3</sub>)<sub>3</sub>), 2.11 (s, 3H COCH<sub>3</sub>). Structure of VB<sub>12</sub>-SA was confirmed using ESI-MS analysis (**Figure 2 c**), ESI-MS (*m/z*): 1478.5 (M+Na)<sup>+</sup>. The results of UV spectra had also confirmed the conjugation of TMC with VB<sub>12</sub>-SA by the characteristic peaks at peak: 278, 361, and 550 nm of VB<sub>12</sub> (**Figure 2 a1, a2, a3**). According to the <sup>1</sup>H NMR spectrum of TMC-SA-VB<sub>12</sub> (**Figure 2 b3**), the characteristic peaks at 7.33, 7.15 ppm for two protons of benzene ring of VB<sub>12</sub> were observed, again indicating the successful conjugation of VB<sub>12</sub>-SA with TMC. Then, the degree of VB<sub>12</sub> substitution was determined by UV spectrophotometer using a calibration curve prepared with standard solutions of VB<sub>12</sub> ( $\lambda = 361 \text{ nm}$ ). Degree of VB<sub>12</sub> substitution was 3.2 % (w/w).

Spectra of HPLC revealed the purity of products (**Figure 3**). VB<sub>12</sub> showed a retention time of 16.131min with peak area of 558.9 under experiment condition, while no peak could be observed in the same position in TMC-SA-VB<sub>12</sub>, implying the successful remove of free VB<sub>12</sub>.





C)

**Figure 2.** The UV and <sup>1</sup>H NMR spectra of VB<sub>12</sub> a1 and b1), TMC a2 and b2) and TMC-SA-VB<sub>12</sub> a3 and b3) and ESI-MS spectra of VB<sub>12</sub>-SA c).

### Characterization of NPs

FITC-INS loaded NPs were prepared by mild ionotropic gelation self-assembly method (20). Different batches of NPs were prepared with different concentrations of TMC, sodium tripolyphosphate, FITC-INS and F68. Formulation was optimized according to parameters including particle size, zeta potential, encapsulating efficiency and drug loading capacity. The results were presented in **Table 1** and **Table 2**. Formulation 3 is adopted as optimal formulation.

Both modified and unmodified NPs had relative spherical morphology as shown in AFM image (**Figure 4**). The characteristics of size, Polydispersity Index (PDI), zeta potential, EE% and DL% of prepared NPs were listed in **Table 3**. Both VB<sub>12</sub>-T NPs and T NPs showed positive charge with relative high EE%.

As the result showed (**Figure 5**), the electrophoretic analysis of the entrapped FITC-INS in both NPs exhibited identical bands as the native FITC-INS, and no additional bands were observed, suggesting the absence of aggregates or fragments. This study indicated that the structure integrity of FITC-INS remained unchanged after drug entrapment.

### Cytotoxicity evaluations of NPs

Cytotoxicity of the NPs and free drug were studied on Caco-2/HT29-MTX cell co-cultures. As demonstrated by the results (**Figure 6**), both NPs exhibited no toxicity at concentration range from 50 to 400 μg/mL (FITC-INS). Also, a cytotoxic compound sodium dodecyl sulfate was used as positive control and showed 0% cell viability after incubation with cells for 4h at a concentration of 50 μg/mL (not presented in Fig 6).

### Uptake study on Caco-2/HT29-MTX cell monolayer

The intracellular uptake of FITC-INS from both VB<sub>12</sub> modified or unmodified NPs were shown in **Figure 7**. All of the test samples exhibited concentration-dependent uptake of FITC-INS. Compared with free FITC-INS solution, both NPs greatly enhanced the drug uptake. Excitingly, further enhanced intracellular uptake was observed for VB<sub>12</sub> modified NPs as compared with the unmodified ones. As shown in **Figure 7a**, the greatest uptake difference between VB<sub>12</sub> modified NPs and unmodified NPs was observed at 300 μg/mL of FITC-INS. Thus, concentration of 300 μg/mL was chosen for the following experiment.

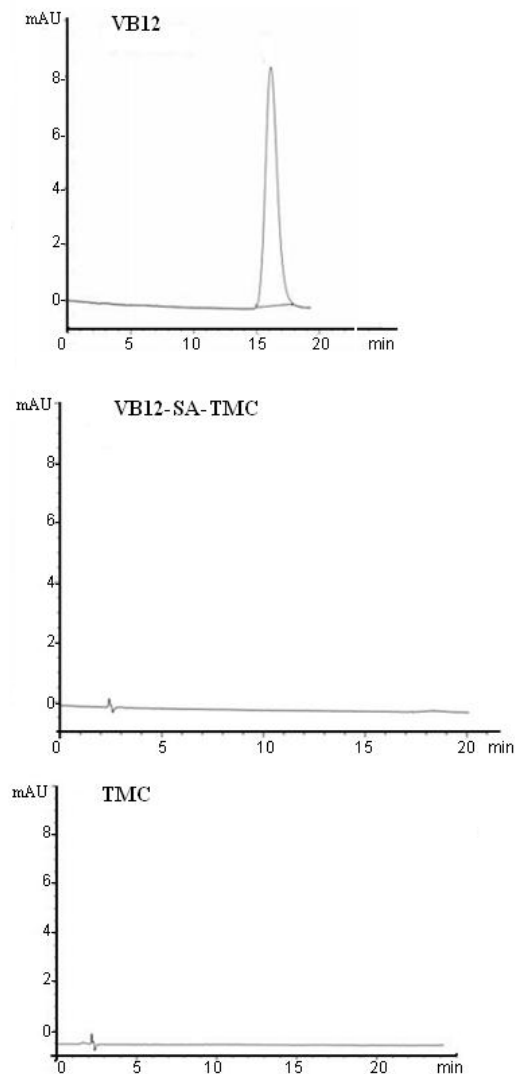


**Figure 3.** HPLC spectra of VB<sub>12</sub>, TMC-SA-VB<sub>12</sub> and TMC.

Cellular uptake of FITC-INS with or without the presence of the mucus was shown in **Figure 7b**. Compared with non-modified NPs, VB<sub>12</sub> modified NPs significantly improved the drug internalization in the presence or in the absence of mucus. Interestingly, both of the NPs exhibited significantly elevated uptake of FITC-INS in the absence of mucus.

Further study of relative uptake mechanisms was conducted. As shown in **Figure 8**, after incubation with sodium chlorate, the cell uptake of both NPs was decreased. Inhibition of chlorpromazine was also observed ( $p < 0.05$ ) on both NPs. However, the additions of filipin was found to inhibit the uptake of VB<sub>12</sub>-T NPs by 39.5% ( $p < 0.05$ ) while there was no effect on

unmodified NPs. Furthermore, the addition of free VB<sub>12</sub> exhibited inhibition of the internalization of VB<sub>12</sub>-T NPs, whereas T NPs kept unaffected, demonstrating the absorption enhancement was due to VB<sub>12</sub> modification.

### Transport study

Based on results of cellular uptake, Caco-2/HT29-MTX co-cultured cell model was used to evaluate the transcellular permeation of NPs by virtue of not only the presence of mucus layer, but also a TEER value close to intestinal epithelium (22). The integrity of the co-cultured cell monolayer was evaluated before the study. Only the cell monolayer with TEER values within the range of 550-650  $\Omega \cdot \text{cm}^2$  was used.

The effect of NPs on tight junction was investigated by monitoring the TEER values of the Caco-2/HT29-MTX cell monolayer. Measured TEER values are presented as the percentage of the initial TEER values (as shown in **Figure 9a**). The two studied NPs exhibited a similar effect on the reduction of TEER value (about 30% reduction). This result indicated that covalent modification of TMC with VB<sub>12</sub> did not change their ability of tight junction opening which plays the key role for the paracellular route of drug transporting.

As shown in **Figure 9b**, the amounts of FITC-INS transported through Caco-2/HT29-MTX cell monolayer were greatly increased with the modification of VB<sub>12</sub> in the presence of mucus ( $p < 0.05$ ). Furthermore, the transported FITC-INS from VB<sub>12</sub> modified NPs were inhibited with the addition of free VB<sub>12</sub> ( $p < 0.05$ ), while T NPs remained unaffected. These result reconfirmed that the VB<sub>12</sub>-specific pathway is involved in the transport of VB<sub>12</sub> modified NPs. Interestingly, even higher transport amounts (1.5-fold) of drug were observed with the VB<sub>12</sub> modified NPs when cells were co-incubated with IF.

Moreover, as expected, higher transport amounts of FITC-INS in the absence of mucus at 2 and 3h ( $p < 0.05$ ) were observed, which was consistent with the results of uptake, demonstrating that the mucus layer acted as a diffusion barrier for NPs. It was reported that the mucus layer may prevent the NPs from reaching and/or adhering to the epithelial cell membrane and then diminish the absorption of NPs (26).

**Table 1.** Content of different formulations (F1, F2...F13).

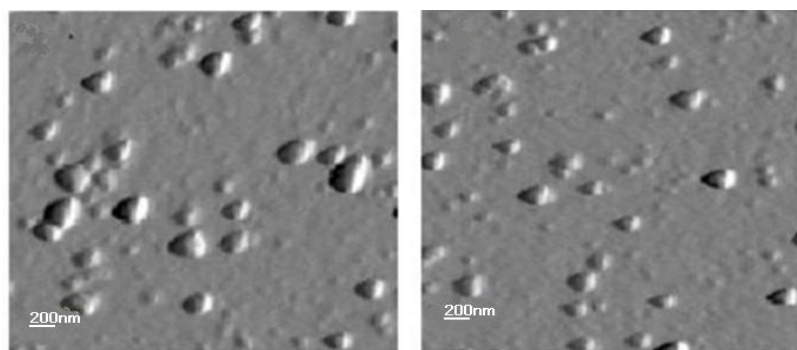
Concentration (mg/mL)	F1	F2	F3	F4	F5	F6	F7	F8	F9	F10	F11	F12	F13
TMC	0.6	0.7	0.8	0.9	0.8	0.8	0.8	0.8	0.8	0.8	0.8	0.8	0.8
TPP	1.0	1.0	1.0	1.0	0.7	0.8	0.9	1.0	1.0	1.0	1.0	1.0	1.0
FITC-INS	1.0	1.0	1.0	1.0	1.0	1.0	1.0	0.6	0.8	1.2	1.0	1.0	1.0
F-68	6.0	6.0	6.0	6.0	6.0	6.0	6.0	6.0	6.0	6.0	2.0	4.0	8.0

**Table 2.** Characterization of formulations (Mean ± SD, n = 3).

Formulations	size(nm)	Zeta potential (mv)	Encapsulation efficiency (%)	Drug loading efficiency (%)
F1	5017.7±341.4	18.9±1.6	97.5±0.5	23.6±0.6
F2	291.2±13.1	20.5±1.8	84.7±0.4	32.1±0.5
F3	196.6±4.0	22.5±0.4	79.6±0.1	33.0±0.4
F4	285.9±1.0	22.7±0.9	72.4±0.4	30.9±0.6
F5	294.4±19.7	14.5±3.4	72.4±0.4	20.3±0.6
F6	274.2±7.1	16.5±0.2	72.3±1.2	27.7±1.7
F7	223.8±0.6	13.7±0.7	75.0±0.3	18.4±0.5
F8	235.8±7.5	19.9±0.2	75.0±0.5	16.8±0.5
F9	222.2±6.2	26.5±0.7	72.6±0.4	18.3±0.2
F10	169.3±1.3	23.3±3.4	75.4±0.5	21.6±1.5
F11	257.5±2.1	25.2±2.87	73.1±0.2	27.6±0.6
F12	209.4±2.4	24.2±1.1	75.5±0.3	32.0±0.8
F13	220.8±2.2	23.1±0.9	78.2±0.3	31.1±1.8

**Table 3.** Characterization of nanoparticles (Mean ± SD, n = 3).

NPs	size (nm)	PDI	Zeta potential (mv)	EE(%)	DL(%)
VB <sub>12</sub> -T NPs	321.4 ± 8.9	0.310 ± 0.023	26.2 ± 0.7	85.7 ± 0.3	34.7 ± 2.1
T NPs	196.6 ± 4.0	0.213 ± 0.005	22.5 ± 0.4	79.6 ± 0.1	33.0 ± 0.4



VB<sub>12</sub>-T NPs

T NPs

**Figure 4.** AFM photographs of VB<sub>12</sub>-T NPs and T NPs.

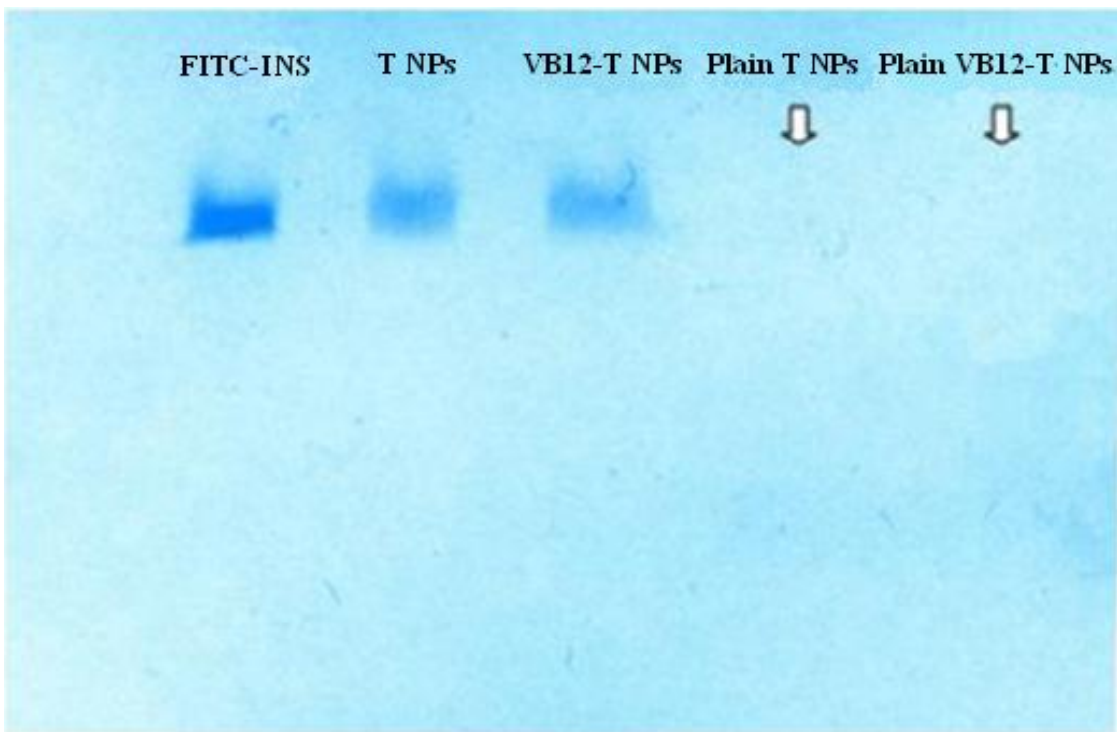


Figure 5. Effect of fabrication technique on the insulin integrity of VB<sub>12</sub>-T NPs and T NPs.

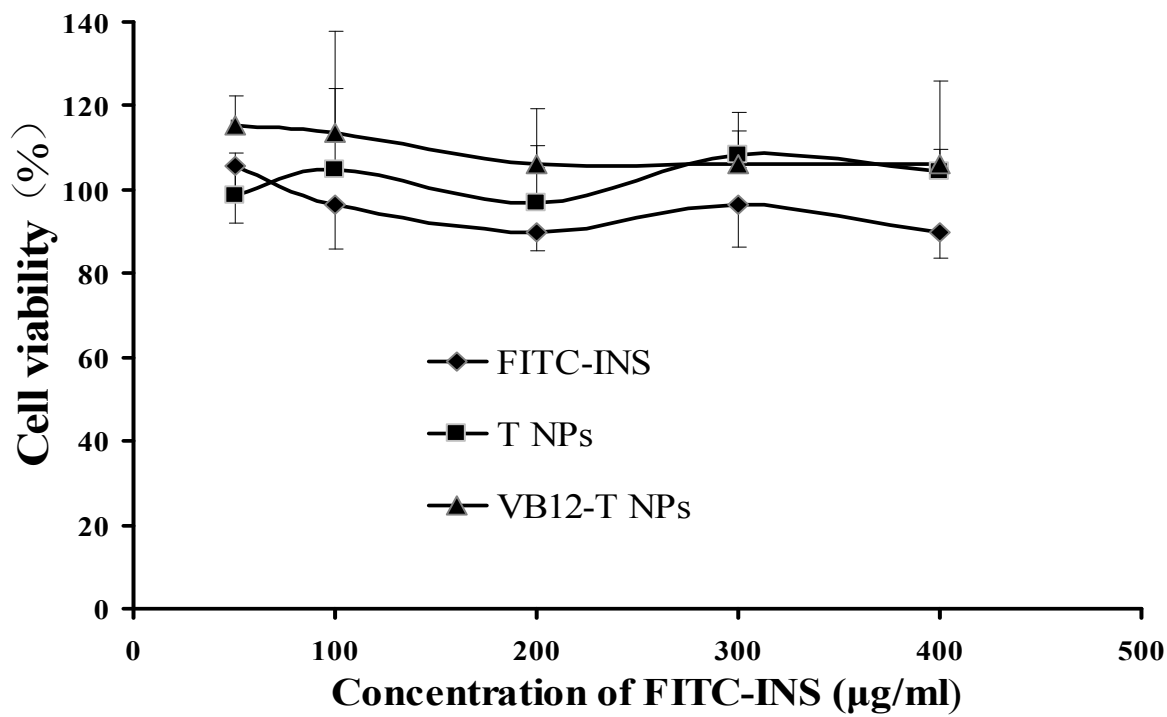
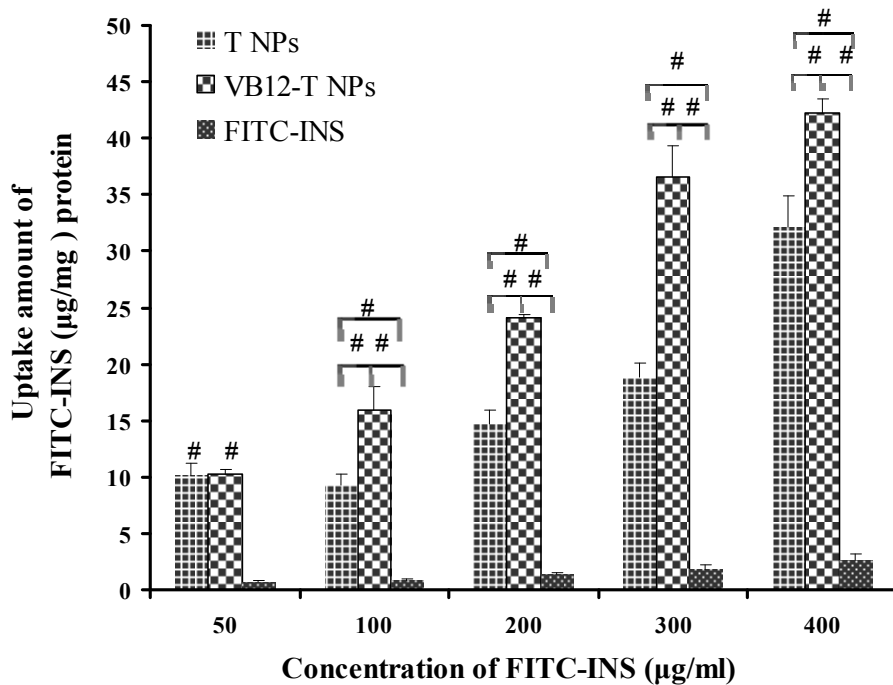
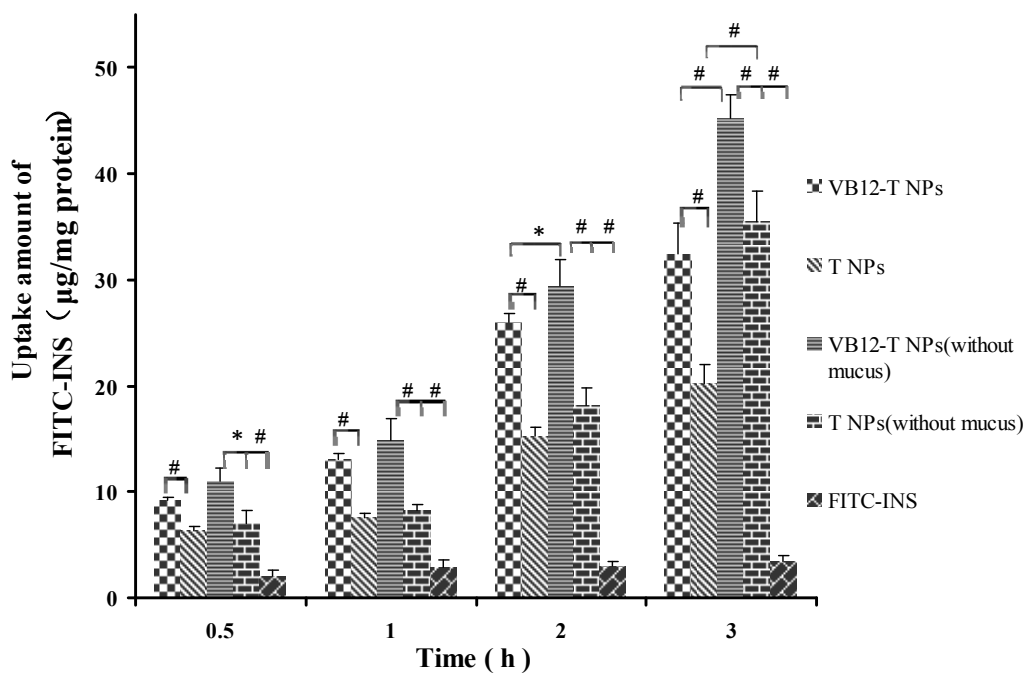


Figure 6. Cell viability of NPs at different concentrations (Mean  $\pm$  SD, n = 3-5).



a)



b)

**Figure 7.** Uptake of VB<sub>12</sub>-T NPs, T NPs and FITC-INS solution by Caco-2/HT29-MTX cells at different concentrations (Mean ± SD, n = 3-4). #: *p* < 0.01. a) and at different time point in the presence or absence of mucus (Mean ± SD, n = 4). \*: *p* < 0.05, #: *p* < 0.01 b).

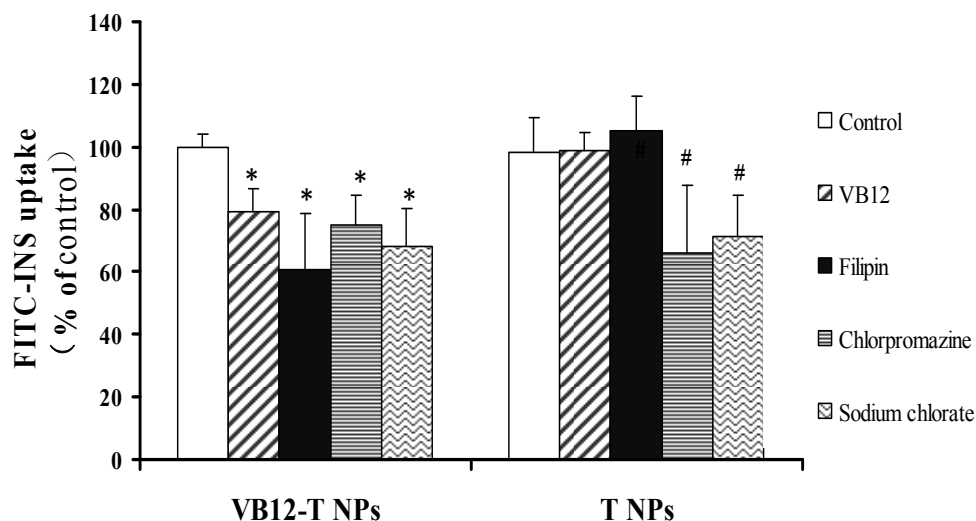


**Figure 8.** Uptake of VB<sub>12</sub>-T NPs and T NPs by Caco-2/HT29-MTX cells at different conditions (Mean  $\pm$  SD, n = 3-4). \*:  $p < 0.05$ , #:  $p < 0.01$ , statistical significance versus control.

Nevertheless, compared to unmodified NPs, VB<sub>12</sub> modified NPs still had higher permeation ability regardless of mucus. Accumulative amounts of transported FITC-INS from VB<sub>12</sub>-T NPs were 3.39-, 2.34-, 2.61-, 2.32-fold higher than that from unmodified NPs in the presence of mucus at every tested time point, respectively, while 1.64-, 1.24-, 1.48-, 1.72-fold higher than unmodified NPs in the absence of mucus at 0.5h, 1h, 2h and 3h. In general, VB<sub>12</sub> modification of NPs can enhance the drug permeation, although it could be partially influenced by mucus layer.

#### Absorption studies in ligated ileum loop

To quantitatively evaluate the *in vivo* absorption of drugs from VB<sub>12</sub> modified NPs, experiments of absorption in ligated intestinal loops model were performed. As shown in **Table 4**, both NPs significantly promoted absorption of FITC-INS, and the drug from T NPs remained in lumen was 1.7-fold higher than VB<sub>12</sub>-T NPs. The amount of FITC-INS from VB<sub>12</sub> modified NPs absorbed by epithelial tissue at 3h was  $9.56 \pm 4.02$   $\mu\text{g/g}$  tissue, 4.8-fold higher than that of unmodified NPs ( $1.97 \pm 0.46$   $\mu\text{g/g}$  tissue). Both of above results could reflect a more efficient *in vivo* absorption of VB<sub>12</sub> modified NPs. To rule out the possibility of counting both absorbed FITC-INS and mucus trapping drugs as fake intake, we removed mucus followed by digestion of tissue to guarantee FITC-INS absorbed by epithelial tissue were counted only.

#### DISCUSSION

In this study, we synthesized TMC and TMC-VB<sub>12</sub> and prepared insulin loaded TMC/TMC-VB<sub>12</sub> nanoparticles. TMC is a quaternized derivative of chitosan, which possesses higher water solubility and stronger positive charge at neutral and basic pH environment. It was reported that even at DQ as low as 10%, increased solubility of TMC can be observed compared with chitosan(27). Besides, stronger positive charge of TMC induced stronger electrostatic interaction between its polymer chain and tight junction of epithelium which may result in higher drug permeation via the paracellular pathway. However, TMC with a very high DQ is hard to be modified, we chose TMC with DQ 16.9%.

To utilize VB<sub>12</sub> as an effective ligand for absorption of NPs, modification of VB<sub>12</sub> should not influence the recognition of VB<sub>12</sub>. Conjugation at the following sites in VB<sub>12</sub> has been reported not to interfere with the ability of the VB<sub>12</sub> transportation: 1) at peripheral propionamide unit on the corrin ring at  $\epsilon$  position, 2) through the phosphate group of the  $\alpha$  "tail", 3) to the 5'-hydroxy group (5' -OH) of the ribose moiety, also in the  $\alpha$  "tail" (8). The 5'-OH group of the ribose moiety of VB<sub>12</sub> was selected as the linking site with TMC using SA as the spacer. The reaction of hydroxyl group with anhydride can produce a free carboxyl which is able to bond to TMC covalently.

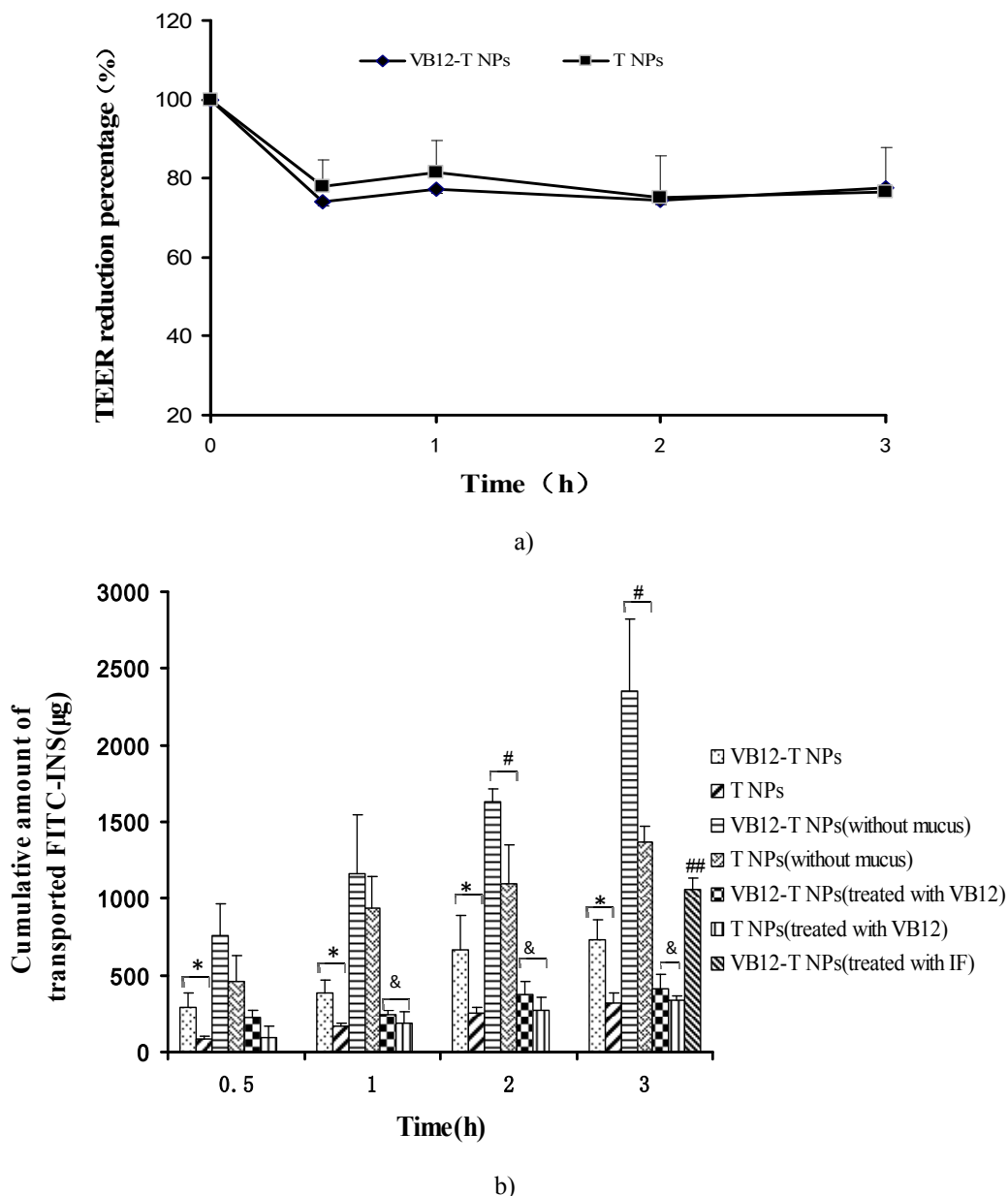


**Figure 9.** Influence of NPs on the TEER of Caco-2/HT29-MTX cell monolayer (Mean ± SD, n = 4) a). transport studies of VB<sub>12</sub>-T NPs and T NPs across the co-incubated Caco-2/HT29-MTX monolayer at different time point in the presence or absence of mucus (Mean ± SD, n = 3-4), \*: *p* < 0.05, Cumulative amounts of transported FITC-INS of VB<sub>12</sub>-T NPs statistical significance versus T NPs; #: *p* < 0.05, Cumulative amounts of transported FITC-INS of VB<sub>12</sub>-T NPs (without mucus) statistical significance versus T NPs (without mucus); &: *p* < 0.01, statistical significance versus T NPs (treated with VB<sub>12</sub>); ##: *p* < 0.01, statistical significance versus VB<sub>12</sub>-T NPs; b).

**Table 4.** Amount of FITC-INS absorbed by epithelial tissue across the mucus layer. (n = 4, Mean ± SD). ##: *p* < 0.01, statistical significance versus T NPs; #: *p* < 0.01, statistical significance versus FITC-INS; \*\*: *p* < 0.01, statistical significance versus T NPs; \*: *p* < 0.01, statistical significance versus T NPs.

Samples	FITC-INS in epithelial tissue (µg/g tissue)	FITC-INS in lumen (µg)
VB <sub>12</sub> -T NPs	9.56 ± 4.02 ##	3.38 ± 0.64 **
T NPs	1.97 ± 0.46 #	5.75 ± 1.09 *
FITC-INS	0.37 ± 0.05	15.93 ± 1.06

The synthesis of TMC-SA-VB<sub>12</sub> was achieved in two steps: firstly, covalent linkage of succinic

anhydride to the 5'-OH group of VB<sub>12</sub>; secondly, the reaction of the linker terminal carboxyl group to the amino groups of TMC.

Most studies use Caco-2 cell model to compare modified and unmodified NPs. Human intestinal Caco-2 cell line, originally obtained from a human colon adenocarcinoma, is the most widely used cell model of intestinal barrier (28-31). It is reported that Caco-2 cells express several morphological and functional characteristics of the mature enterocytes. However, the Caco-2 cells possess no mucus layer, which differs from the *in vivo* condition of intestinal epithelium. Since mucus may greatly influence the behavior of the nanoparticles and even ligand binding efficacy (4), *in vitro* evaluation of ligand modified NPs on a mucus producing cell model would offer more relevant results. Goblet cells, the second largest population of epithelial cells, account for 10-24% of the intestinal epithelial cells, are responsible for the mucus production in the GI tract. In the present study, Caco-2/HT29-MTX co-cultured cell model was used, which consists of both absorptive enterocyte-like Caco-2 cells and the mucus-producing goblet cell-like HT29-MTX cells. It is also confirmed that both of them have an IF-dependent fashion (32-35) and IF-independent fashion (29, 36-37) for the transportation of VB<sub>12</sub>. Also, this cell model could be affected by some chemical reagent. To study the different mechanism of cell uptake and transport between the two NPs, we pre-incubated cell models with given agentia. Sodium chlorate is an inhibitor of glycosaminoglycan sulfation which could remove anionic sites on the apical membrane thus leading to reduction of interaction between positive charged TMC and negative charged cell membrane (39). Chlorpromazine could disrupt the assembly and disassembly of clathrin at a concentration of 6-10 mg/mL and filipin is known to disrupt caveolae structure by binding to cholesterol and disorganizing the caveolin (26). Also VB<sub>12</sub> was used to study competitive mechanism, results of uptake mechanism indicated that enhancement of cellular uptake of VB<sub>12</sub> modified NPs was due to the VB<sub>12</sub> mediated interaction, which may be involved in the caveolae and clathrin-mediated endocytosis pathway. Studies showed that both IF, salivary haptocorrin and their receptors could be found in Caco-2 cells and proved an IF dependent manner for VB<sub>12</sub> transportation (32, 40), addition of IF lead to a higher transport of VB<sub>12</sub> modified NPs, Therefore, we can conclude that an IF-dependent fashion was involved in specific transporting

pathway of VB<sub>12</sub> modified NPs.

It is interesting to see a lower amount of uptake with the presence of mucus, it may be due to the impeding or trapping of NPs and this phenomenon was also observed by other researchers (38). However, it has to be mentioned that a contrary result was reported in an early study of our group, in which a less positively charged NPs was used (4). The same phenomenon was observed in transport study, confirmed what we expected.

However, the behavior of NPs in intestine may be affected by many physiological factors, we designed *in vivo* experiment with rat intestine, and more study of pharmacodynamics and pharmacokinetics should be further conducted.

## CONCLUSION

In the present work, VB<sub>12</sub> modified TMC NPs were prepared and characterized. Compared with unmodified NPs, VB<sub>12</sub> modified NPs showed significantly higher drug internalization in Caco-2/HT29-MTX cell model. The internalization mechanism via VB<sub>12</sub> mediation included caveolae and clathrin-mediated endocytosis pathway. Meanwhile, an increased transportation of drugs was observed for VB<sub>12</sub> modified NPs, possibly due to ligand-receptor interaction via an IF-dependent manner. Moreover, influence of mucus on the performance of NPs was investigated. VB<sub>12</sub>-T NPs could enhance the drug permeation with or without the presence of mucus layer, though, by which the targeting property could be partially reduced. Finally, the VB<sub>12</sub> modification could promote the absorption of NPs in ligated ileum loop model than unmodified NPs. All of the results suggested that VB<sub>12</sub> could be used as a promising ligand for oral delivery of peptides and proteins.

## ACKNOWLEDGMENTS

The authors acknowledge financial support from the National Natural Science Foundation of China (81173010) and State Key Laboratory of Long-acting and Targeting Drug Delivery System.

## REFERENCES

1. Bakhru SH, Furtado S, Morello AP, Mathiowitz E. Oral delivery of proteins by biodegradable nanoparticles. *Adv Drug Delivery Rev.* 2013;65: 811-821.
2. Muller G. Oral delivery of protein drugs: driver for

- personalized medicine. *Curr Issues Mol Biol* 2011;13: 13-24.
3. Yun Y, Cho YW, Park K. Nanoparticles for oral delivery: targeted nanoparticles with peptidic ligands for oral protein delivery. *Adv Drug Delivery Rev.* 2013;65: 822-832.
  4. Jin Y, Song Y, Zhu X, Zhou D, Chen C, Zhang ZR, Huang Y. Goblet cell-targeting nanoparticles for oral insulin delivery and the influence of mucus on insulin transport. *Biomaterials.* 2012;33: 1573-1582.
  5. Pridgen EM, Alexis F, Kuo TT, Levy-Nissenbaum E, Karnik R, Blumberg RS, Langer R, Farokhzad OC. Transepithelial transport of Fc-targeted nanoparticles by the neonatal fc receptor for oral delivery. *Sci Transl Med.* 2013;5: 213ra167.
  6. des Rieux A, Pourcelle V, Cani PD, Marchand-Brynaert J, Preat V. Targeted nanoparticles with novel non-peptidic ligands for oral delivery. *Adv Drug Delivery Rev.* 2013;65: 833-844.
  7. Kavimandan NJ, Losi E, Peppas NA. Novel delivery system based on complexation hydrogels as delivery vehicles for insulin-transferrin conjugates. *Biomaterials.* 2006;27: 3846-3854.
  8. Petrus AK, Fairchild TJ, Doyle RP. Traveling the vitamin B<sub>12</sub> pathway: oral delivery of protein and peptide drugs. *Angew Chem.* 2009;48: 1022-1028.
  9. Nicolas JP, Gueant JL. Gastric intrinsic factor and its receptor. *Bailliere's clinical haematology.* 1995;8: 515-531.
  10. Okuda K. Discovery of vitamin B<sub>12</sub> in the liver and its absorption factor in the stomach: a historical review. *J Gastroenterol Hepatol.* 1999;14: 301-308.
  11. Habberfield A, Jensen-Pippo K, Ralph L, Westwood SW., Russell-Jones GJ. Vitamin B<sub>12</sub>-mediated uptake of erythropoietin and granulocyte colony stimulating factor in vitro and in vivo. *Int J Pharm.* 1996;145: 1-8.
  12. Russell-Jones GJ, Westwood SW, Farnworth PG, Findlay JK, Burger HG. Synthesis of LHRH antagonists suitable for oral administration via the vitamin B<sub>12</sub> uptake system. *Bioconjugate Chem.* 1995;6: 34-42.
  13. Russell-Jones GJ, Westwood SW, Habberfield AD. Vitamin B<sub>12</sub> mediated oral delivery systems for granulocyte-colony stimulating factor and erythropoietin. *Bioconjugate Chem.* 1995; 6: 459-465.
  14. Chalasani KB, Russell-Jones GJ, Yandrapu SK, Diwan PV, Jain SK. A novel vitamin B<sub>12</sub>-nanosphere conjugate carrier system for peroral delivery of insulin. *J Controlled Release.* 2007;117: 421-429.
  15. Chen F, Zhang ZR, Huang Y. Evaluation and modification of N-trimethyl chitosan chloride nanoparticles as protein carriers. *Int J Pharm.* 2007;336: 166-173.
  16. Jintapattanakit A, Junyaprasert VB, Mao S, Sitterberg J, Bakowsky U, Kissel T. Peroral delivery of insulin using chitosan derivatives: a comparative study of polyelectrolyte nanocomplexes and nanoparticles. *Int J Pharm.* 2007;342: 240-249.
  17. Yin L, Ding J, He C, Cui L, Tang C, Yin C. Drug permeability and mucoadhesion properties of thiolated trimethyl chitosan nanoparticles in oral insulin delivery. *Biomaterials.* 2009;30: 5691-5700.
  18. Sieval AB, Thanou M, Kotze' AF, Verhoef JC, Brussee J, Junginger HE. Preparation and NMR characterization of highly substituted N-trimethyl chitosan chloride. *Carbohydr Polym.* 1998; 36: 157-165.
  19. Francis MF, Cristea M, Winnik FM. Exploiting the vitamin B<sub>12</sub> pathway to enhance oral drug delivery via polymeric micelles. *Biomacromolecules.* 2005;6: 2462-2467.
  20. Wang S, Jiang T, Ma M, Hu Y, Zhang J. Preparation and evaluation of anti-neuroexcitation peptide (ANEP) loaded N-trimethyl chitosan chloride nanoparticles for brain-targeting. *Int J Pharm.* 2010;386: 249-255.
  21. Sonvico F, Cagnani A, Rossi A, Motta S, Di Bari MT, Cavatorta F, Alonso MJ, Deriu A, Colombo P. Formation of self-organized nanoparticles by lecithin/chitosan ionic interaction. *Int J Pharm.* 2006;324: 67-73.
  22. Hilgendorf C, Spahn-Langguth H, Regardh CG, Lipka E, Amidon GI, Langguth P. Caco-2 versus Caco-2/HT29-MTX co-cultured cell lines: permeabilities via diffusion, inside- and outside-directed carrier-mediated transport. *J Pharm Sci.* 2000;89: 63-75.
  23. Mislick KA, Baldeschwieler JD. Evidence for the role of proteoglycans in cation-mediated gene transfer. *Proc Natl Acad Sci U. S. A.* 1996;93: 12349-12354.
  24. Rejman J, Bragonzi A, Conese M. Role of clathrin- and caveolae-mediated endocytosis in gene transfer mediated by lipo- and polyplexes. *Mol Ther.* 2005;12: 468-474.
  25. Ould-Ouali L, Arien A, Rosenblatt J, Nathan A, Twaddle P, Matalenas T, Borgia M, Arnold S, Leroy D, Dinguizli M, Rouxhet L, Brewster M, Preat V. Biodegradable self-assembling PEG-copolymer as vehicle for poorly water-soluble drugs. *Pharm Res.* 2004;221: 1581-1590.
  26. Kotze AF, Luessen HL, de Leeuw BJ, de Boer AG, Verhoef JC, Junginger HE. Comparison of the effect of different chitosan salts and N-trimethyl chitosan chloride on the permeability of intestinal epithelial cells (Caco-2). *J Controlled Release.* 1998;51: 35-46.
  27. Artursson P, Borchardt RT. Intestinal drug absorption and metabolism in cell cultures: Caco-2 and beyond. *Pharm Res.* 1997;14: 1655-1658.
  28. Bose S, Seetharam S, Dahms NM, Seetharam B.

- Bipolar functional expression of transcobalamin II receptor in human intestinal epithelial Caco-2 cells. *J Biol Chem.* 1997;272: 3538-3543.
29. Chen C, Fan T, Jin Y, Zhou Z, Yang Y, Zhu X, Zhang ZR, Zhang Q, Huang Y. Orally delivered salmon calcitonin-loaded solid lipid nanoparticles prepared by micelle-double emulsion method via the combined use of different solid lipids. *Nanomedicine.* 2013;8: 1085-1100.
  30. Zhu X, Shan W, Zhang P, Jin Y, Guan S, Fan T, Yang Y, Zhou Z, Huang Y. Penetratin derivative-based nanocomplexes for enhanced intestinal insulin delivery. *Mol Pharm.* 2014;11: 317-328.
  31. Adkins Y, Lonnerdal B. Mechanisms of vitamin B(12) absorption in breast-fed infants. *J Pediatr Gastroenterol Nutr.* 2002;35: 192-198.
  32. Gueant JL, Masson C, Schohn H, Girr M, Saunier M, Nicolas JP. Receptor-mediated endocytosis of the intrinsic factor-cobalamin complex in HT 29, a human colon carcinoma cell line. *FEBS Lett.* 1992;297: 229-232.
  33. Russell-Jones GJ, Arthur L, Walker H. Vitamin B12-mediated transport of nanoparticles across Caco-2 cells. *Int J Pharm.* 1999;179: 247-255.
  34. Schohn H, Gueant JL, Girr M, Nexo E, Baricault L, Zweibaum A, Nicolas JP. Synthesis and secretion of a cobalamin-binding protein by HT 29 cell line. *Biochem J.* 1991;280 ( Pt 2): 427-430.
  35. Bose S, Kalra S, Yammani RR, Ahuja R, Seetharam B. Plasma membrane delivery, endocytosis and turnover of transcobalamin receptor in polarized human intestinal epithelial cells. *J Physiol.* 2007;581: 457-466.
  36. Pons L, Guy M, Lambert D, Hatier R, Gueant J. Transcytosis and coenzymatic conversion of [(57)Co]cobalamin bound to either endogenous transcobalamin II or exogenous intrinsic factor in caco-2 cells. *Cell Physiol Biochem.* 2000;10: 135-148.
  37. Schipper NG, Olsson S, Hoogstraate JA, de Boer AG, Varum KM, Artursson P. Chitosans as absorption enhancers for poorly absorbable drugs 2: mechanism of absorption enhancement. *Pharm Res.* 1997; 14: 923-929.
  38. Behrens I, Pena AI, Alonso MJ, Kissel T. Comparative uptake studies of bioadhesive and non-bioadhesive nanoparticles in human intestinal cell lines and rats: the effect of mucus on particle adsorption and transport. *Pharm Res.* 2002;19: 1185-1193.
  39. Huang M, Ma Z, Khor E, Lim LY. Uptake of FITC-chitosan nanoparticles by A549 cells. *Pharm Res.* 2002;19: 1488-1494.
  40. Alpers DH, Russell-Jones GJ. Gastric intrinsic factor: the gastric and small intestinal stages of cobalamin absorption. a personal journey. *Biochimie.* 2013;95: 989-994